Proceedings of ASME Turbo Expo 2015: Turbine Technical Conference and Exposition
GT2015
June 15 – 19, 2015, Montréal, Canada

GT2015-43803

DEMONSTRATED OPERABILITY AND RELIABILITY IMPROVEMENTS FOR A PROTOTYPE HIGH-SPEED ROTARY-DISC ATOMIZER SUPPORTED ON ACTIVE MAGNETIC BEARINGS

Rasish K. Khatri
Calnetix Technologies
Cerritos, California, USA

Lawrence A. Hawkins
Calnetix Technologies
Cerritos, California, USA

Claude Bazergui
Dedert Corporation
Homewood, Illinois, USA

ABSTRACT

A state-of-the-art, rotary-disc atomizer driven by a permanent-magnet electric motor and supported by active magnetic bearings (AMB) was designed, fabricated, and tested as part of a spray-dryer system within a pharmaceutical-processing plant. The atomizing process imposed several challenges on the AMBs, including large, highly-dynamic rotor imbalances and large, quasi-periodic external radial impulses. Several design changes were systematically implemented to mitigate the effects of large rotor imbalances. A novel impulse detection and recovery system was introduced to alleviate the effects of external impulses. These changes, which have steadily improved the operability and reliability of the machine, are described here along with field test data.

INTRODUCTION

Spray-drying is the preferred method by which the pharmaceutical-processing and food-processing industries produce various dry powders and particles. Figure 1 shows a process flow diagram for a spray-dryer. In a typical spray-drying application, a slurry or solution liquid is fed into a nozzle, which breaks up the fluid into a spray. The nozzle, often a rotary-disc atomizer, creates equal-size droplets. The size of the droplets is inversely proportional to the nozzle/disc peripheral speed; a larger diameter and a higher speed typically yield smaller particle sizes.

A hot stream of gas, usually air or nitrogen, rapidly dries the droplets to produce equal-size dry powders and particles. The particles produced in modern spray-drying applications typically have a diameter ranging from 0.0039-0.0079 in. (0.1-0.2 mm).

Existing rotary-disc atomizers are generally driven by a standard motor connected to a belt drive or gearbox, supported by oil-lubricated spindle bearings. This technology has several drawbacks: (1.) the maximum tip speed of the disc (and thus the minimum particle size) is lower than desired for some applications and (2.) the technology requires regular maintenance with significant process downtime, mainly due to the need to service the bearings and the oil-lubrication system.

This paper introduces an innovative new 250 kW Magnetic Spray Machine (MSM-250), which eliminates these problems by using a high-speed, permanent-magnet AC electric motor and active magnetic bearings (AMBs). This largely frictionless design allows for higher maximum disc speeds and reduced overall maintenance. The MSM-250 has a maximum continuous operating speed of 16,000 rpm with a 12.75 in. (32.39 cm) diameter disc mounted directly to the motor shaft [1].

The first field-test unit of the MSM-250 was placed in a spray dryer used for the production of pharmaceutical dry powders. The required nominal operating speed range for the

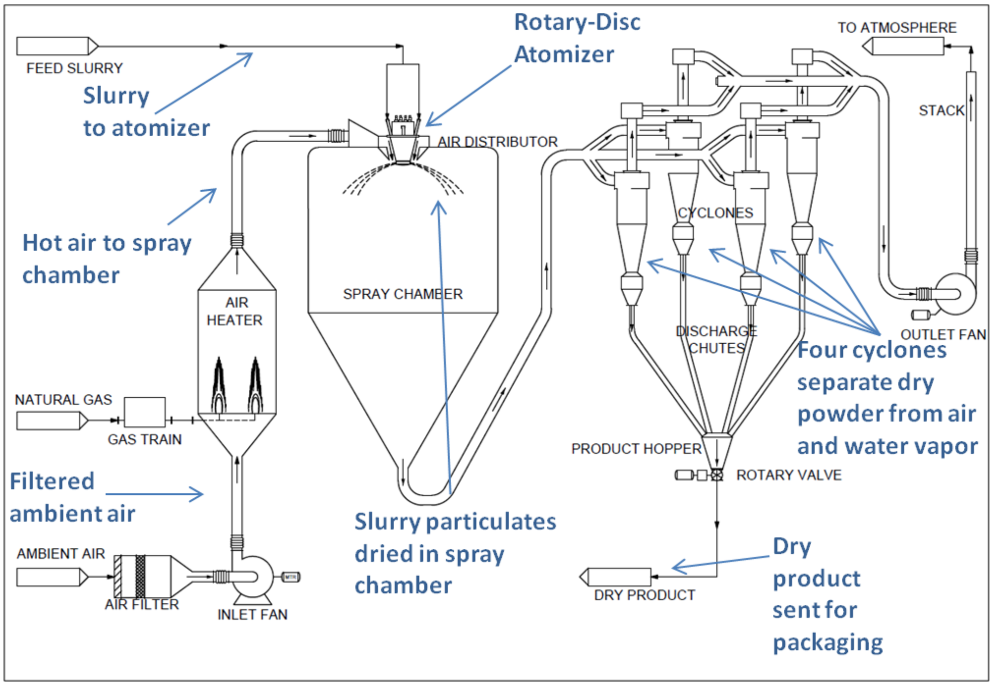

Figure 1. Process flow diagram for the spray-drying application.

MSM-250 in this application is 12,000-13,000 rpm. While the vast majority of the applications for the MSM-250 will use a slurry with a dynamic viscosity less than 1 Pa-s, this particular application uses a slurry with a dynamic viscosity greater than 30 Pa-s.

Figure 2 shows an overview of the atomizer well, the location where the atomizer is installed above the spray chamber. Slurry enters the atomizer housing through two feed tubes, located at the top of the atomizer housing. The feed tubes are connected to a feed distributor, which uniformly feeds the slurry into the disc center annulus. The disc is located at the bottom of the atomizer and exposed to the spray chamber. The particles of slurry exit the atomizer disc radially through the 48 slots milled along the disc's perimeter. An air distributor sends hot air (approximately 780^{o}F/415^{o}C) into the atomizer chamber to quickly dry the slurry droplets exiting from the atomizer disc.

During typical startup of the spray dryer, the atomizer is spun up to the desired speed in air. Next, water is delivered to the atomizer disc through the feed tubes at steadily increasing feed rates.

After that, slurry is delivered to the disc in increasing quantities and at increasing feed rates, and the concentration of pure water is steadily decreased.

Once the nominal concentration of slurry has been achieved, the feed rate and concentration are kept at a steady level.

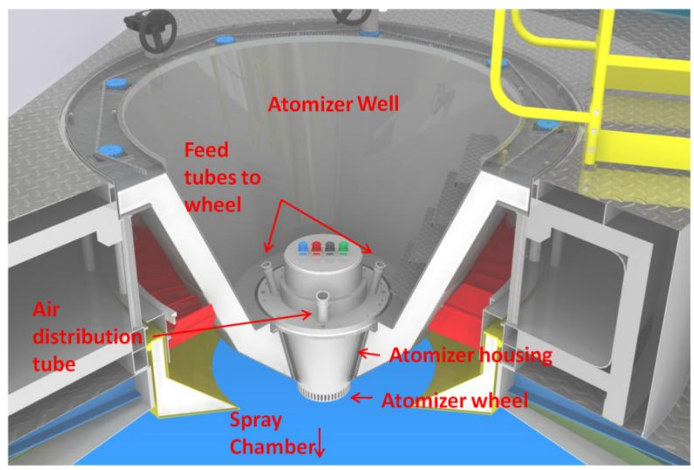

Figure 2. Overview of the atomizer well

The original AMB design requirements for the MSM-250 assumed an even distribution of a well-mixed slurry across the atomizer disc. However, during initial field commissioning of the MSM-250, several previously-unknown process-related factors hindering the successful, continuous operation of the AMBs were discovered. Suspected factors included material buildup on the atomizer disc and large masses of quasi-solid slurry passing to the disc. This paper describes these problems in detail and discusses the design changes and corrective actions implemented by the magnetic bearing developers to resolve these issues.

DESIGN OVERVIEW

Figure 3 shows a cross-section of the MSM-250. The rotor is supported by a radial AMB assembly near the lower-end of the rotor and a combination radial/axial AMB assembly near the upper-end of the rotor. As mentioned earlier, the atomizer disc is attached to the bottom of the shaft, and slurry is fed directly into the disc through two feed tubes.

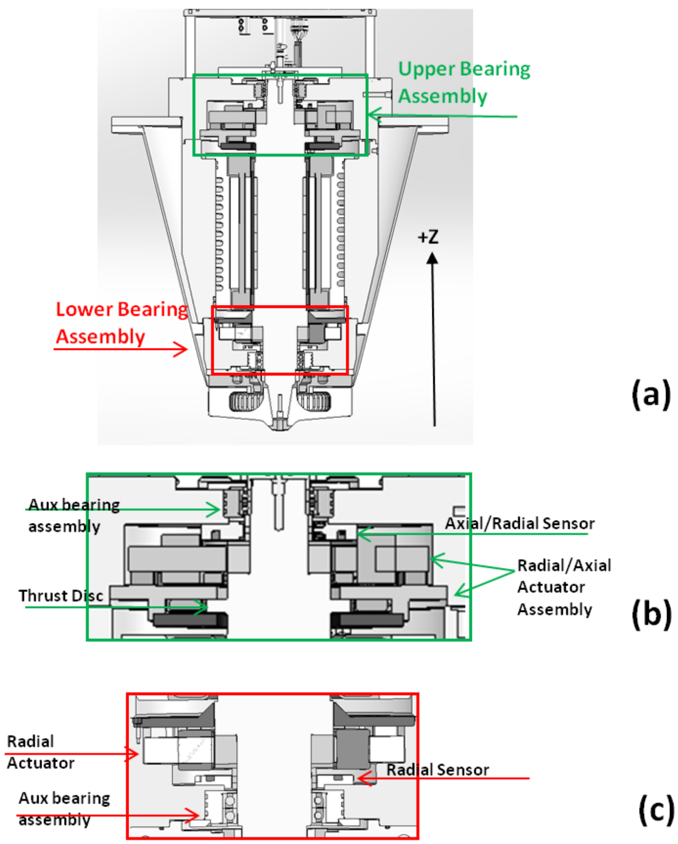

Figure 3. (a) Cross-section of the MSM-250, (b) detailed view of the upper AMBs and auxiliary bearings, and (c) detailed view of the lower AMBs and auxiliary bearings

Each AMB assembly consists of a permanent-magnet-biased, homopolar electromagnetic-actuator assembly and a reluctance position-sensor assembly. The AMB assembly supporting the lower end of the rotor senses and corrects for position errors in two orthogonal radial directions (*x1*- and *y1*-directions). The AMB assembly supporting the upper end of the rotor controls the rotor position in two orthogonal radial directions (*x2*- and *y2*- directions) and the axial direction (*z*-direction). In total, there are five axes of control. Refs. [2]-[4] describe the basic design of the actuators and sensors used in this machine. Table 1 summarizes the nominal load capacities of the AMBs.

Due to preliminary project scheduling, budget, and planning, the original development plan did not call for the development of a new motor, AMBs, or auxiliary bearings. As such, a previously-used motor supported by AMBs was employed in this design.

Table 1. Measured load capacities of all AMBs

	Lower Radial	Upper Radial	Axial
Load Capacity (lbf)	275	325	700

Outboard of the sensors and actuators on both ends of the machine are the auxiliary bearings. There is a duplex pair of auxiliary bearings on each end of the rotor. The auxiliary bearings are intended to bear the loads of the rotor if a) power is turned off, b) there is a component failure, or c) the AMBs lose control of the rotor for any reason. When the rotor is levitated, the radial auxiliary bearing clearance is ±0.005 inches (±0.127 μm) and the axial clearance is ±0.0065 inches (±0.165 μm). Three o-rings are placed around the auxiliary bearing housing to reduce the total radial stiffness of the auxiliary bearing. The auxiliary bearings are designed to withstand 10 rotor drops with a spindown from 16,000 rpm to zero rpm on the auxiliary bearings.

In the original design of the MSM-250 (V0), both the upper and lower auxiliary bearing pairs were 60 mm hybrid-ceramic, angular-contact ball bearings. In the latest version of the MSM-250 (V1), an 80 mm auxiliary bearing is used on the lower end of the machine. The reason behind this change is explained in the DESIGN IMPROVEMENTS section.

The position sensor electronics, power amplifiers used to drive current through the actuator coils, digital-signal-processing (DSP) control board, and other supporting hardware are contained within a Magnetic Bearing Controller (MBC). The MBC is capable of controlling signals with frequencies up to 2,000 Hz.

As mentioned above, the MBC is able to actively sense and control the rotor position in four radial axes and one axial axis. Figure 4 shows a simplified SISO (Single Input, Single Output) control loop for the AMBs. AMBs can be treated similarly to conventional bearings with a complex dynamic stiffness that has a more complicated frequency dependence. The AMB dynamic stiffness is the ratio of the change in output force of the actuator to the change in sensed rotor displacement. Note that the actuator and sensor are not collocated, meaning that the axial plane in which the magnetic force acts is not the same as the axial plane in which the sensor observes the rotor motion. Ref. [5] reviews the basic terminology and nomenclature used in characterizing the performance of an AMB.

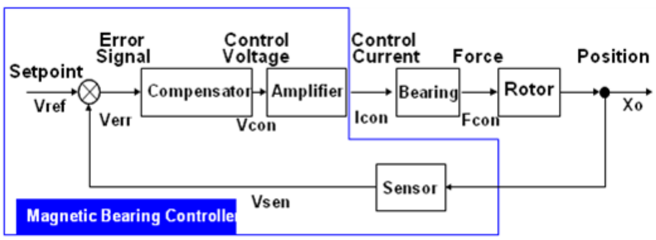

Figure 4. Control loop used to control the rotor position to a given setpoint

Figure 5 shows the measured plant frequency response in the *x1*- and *x2*- directions at 13,000 rpm for the MSM-250 V0 design. The plant gain is the sensor output divided by the input command to the amplifier. The plant gain includes the dynamics of the amplifier, actuator, rotor, and sensor. As seen in the figure, the first backward-whirl bending mode frequency (240 Hz) is fairly close to the operating speed of the rotor (208-217 Hz). The spin frequency shown in the figure is 216 Hz. The 1st forward-whirl bending mode frequency is 477 Hz. The plant gains at the first two bending modes are significantly larger at the upper bearing than at the lower bearing. This is because the first two bending modes have larger modal deflections at the upper bearing sensor and actuator locations relative to the lower bearing.

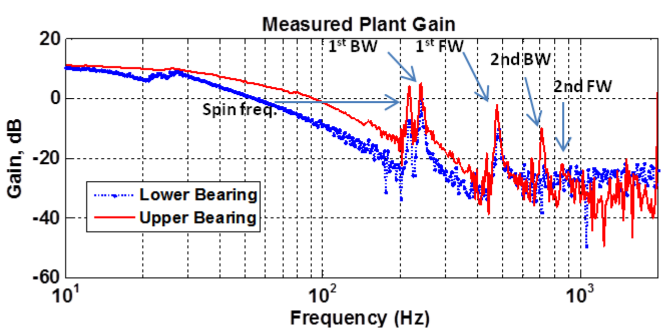

Figure 5. Measured radial plant frequency response at 13,000 rpm for the MSM-250 V0

A complete dynamic model of the rotor and AMBs was created using an internally-developed solver. The basic modeling approach used by the solver is described in Ref [6]. The predicted first and second forward-whirl bending mode shapes at 13,000 rpm are shown in Figure 6. The first bending mode is heavily driven by the stiffness of the lower bearing section, as well as the mass/inertia properties of the disc.

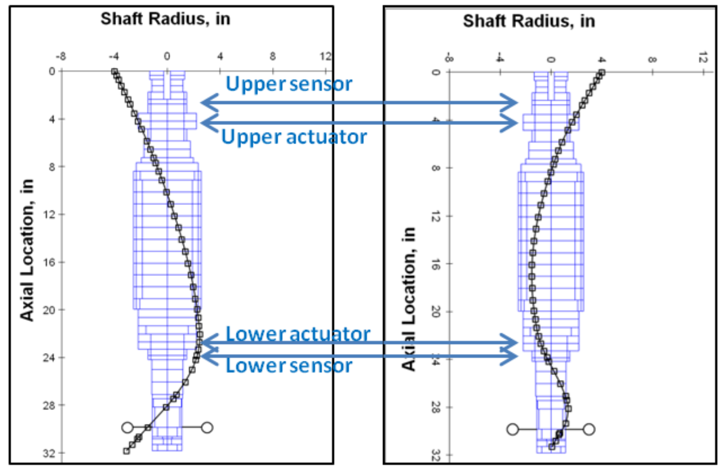

Figure 6. First (left) and second (right) forward-whirl bending modes at 13,000 rpm for the MSM-250 V0 design

Figure 7 shows the AMB stiffness and damping at 13,000 rpm for the lower-radial and upper-radial bearings. The AMB has positive damping up to 75 Hz at the lower bearing and up to 100 Hz at the upper bearing. The positive damping in this frequency range is used to stabilize the rigid-body modes. The low-frequency (10-20 Hz) stiffness at the upper bearing is approximately 17,500 lbf/in (3,640,000 N/m), and the low-frequency stiffness at the lower bearing is approximately 20,000 lbf/in (3,503,000 N/m).

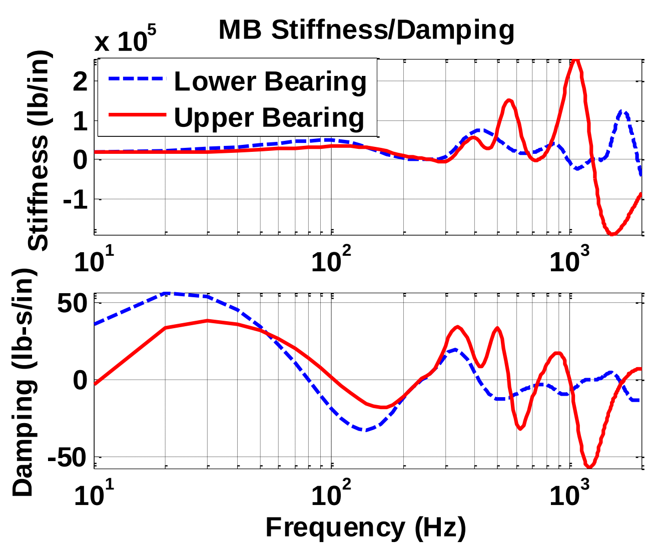

Figure 7. Calculated radial AMB stiffness and damping at 13,000 rpm for the MSM-250 V0

Figure 8 shows the measured closed-loop response of the rotor-bearing system at 13,000 rpm. The closed-loop response was measured with the rotor spinning in air. The closed loop response at the upper bearing is larger than that of the lower bearing, because the AMB stiffness for the upper bearing is smaller than that of the lower bearing.

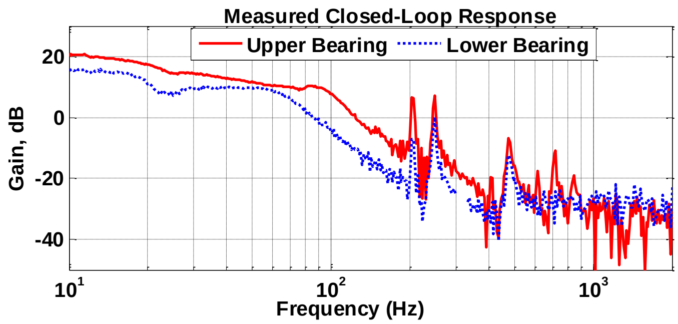

Figure 8. Measured radial closed-loop response at 13,000 rpm for the MSM-250 V0

FIELD-TESTING

The first MSM-250 V0 field-test unit was commissioned in August 2012. Several problems were observed during initial field testing.

Figure 9 shows the radial position orbit plots for the lower and upper radial bearings during typical three-minute time windows taken during an air run and a slurry run. The slurry produces significantly larger rotor motion, especially at the lower bearing. For the air run, the observed rotor motion is mostly synchronous, caused by rotor unbalance and sensor runout. For the slurry run, the observed rotor motion is contains both synchronous and low-frequency (<20 Hz) content. The synchronous motion is due to rotor unbalance, sensor runout, and unbalance due to slurry buildup on the disc. The transients are attributed to forces imparted by the slurry to the disc.

The synchronous amplitude and phase of the atomizer varied with time during normal operation at a steady speed and flow rate. Figure 10 shows the synchronous amplitude on the upper and lower bearings, during a 24-hour run. The synchronous amplitudes range from 0.0004 to 0.0018 inches (10.2 to 45.7 μm) on the lower bearing, and 0.0001 to .0015 inches (2.54 to 38.1 μm) on the upper bearing, depending on the process conditions. The change in balance condition of the disc with time was due to uneven build-up and discharge of solid deposits on the disc.

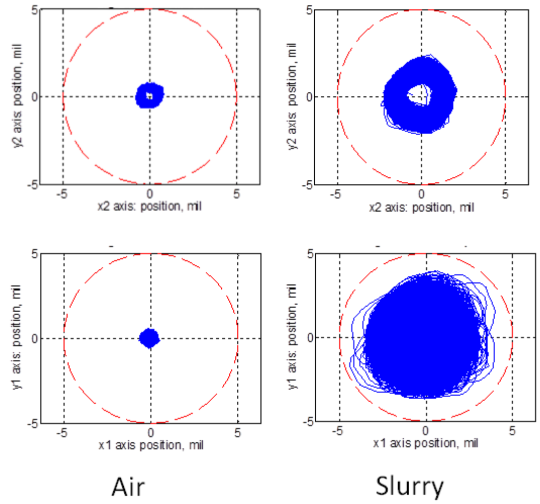

Figure 9. Position orbits for the lower bearing (bottom) and upper bearing (top) during 3-minute air run (left) and 3-minute slurry run (right)

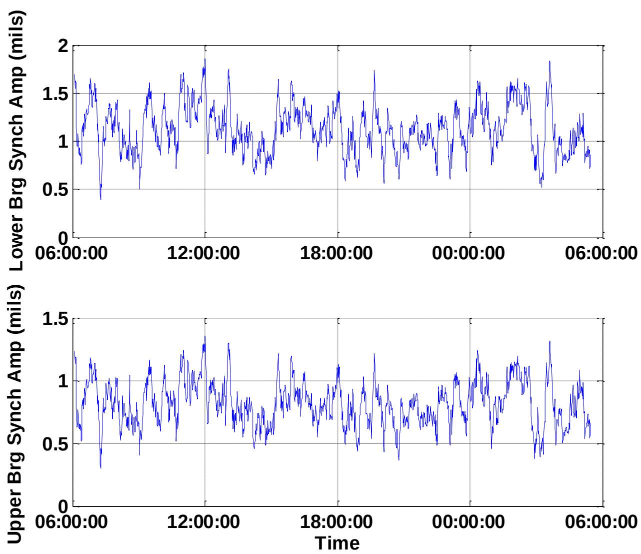

Figure 10. Synchronous position amplitude on the upper and lower bearings over 24 hours

Process-Related Radial/Torsional Impulses

During an initial run of the MSM-250, the atomizer spun for approximately 2 hours on slurry prior to tripping an excessive vibration fault limit detected by the lower radial position sensors. The unit was started up again shortly after the fault. Once again, the unit tripped an excessive vibration fault limit at the lower bearing after approximately 4.5 hours of running on slurry. An examination of the data revealed that the excessive vibration faults were caused by a loss of control at both radial bearings after the rotor contacted the lower auxiliary bearing. This resulted in a rotor drop and subsequent coast down from 13,000 rpm to 0 rpm on the auxiliary bearings.

Figure 11(a) shows the rotor position magnitude during a 30-second time interval taking place directly before, during, and after a rotor drop event. Figure 11(b) shows the portion of Figure 11(a), from 11.9 to 12.5 seconds. A large radial impulse occurs at approximately 12.33 seconds in the figure, and is primarily seen by the lower bearing sensor. For several seconds prior to the radial impulse, the rotor-bearing system is stable, but there is large synchronous and low-frequency rotor displacement seen by the lower sensor. In the 0.15 seconds directly prior to the radial impulse, there are two smaller radial impulses that increase the position of the rotor beyond 0.0004 inches (102 μm). After the radial impulse, the lower AMB is able to stabilize the rotor motion. However, after the rotor contacts the lower auxiliary bearings, at approximately 12.30 seconds, the rotor contacts the upper auxiliary bearings, and the upper bearing is no longer able to stably control the rotor motion. The frequency content of the upper bearing displacement after contact with the auxiliary bearing shows large synchronous motion and large motion in the 150-170 Hz frequency range.

To help explain this phenomenon, the effective stiffness of the auxiliary bearings and o-rings was incorporated into the rotor-magnetic bearing model. The stiffness of the o-rings was estimated using published test data [7]. Figure 12 shows the resulting predicted plant transfer function magnitude of the rotor supported by the AMBs and the auxiliary bearings. The plant transfer function shows four rigid-body modes between 100 Hz and 200 Hz, including modes at 150 Hz and 188 Hz. The predicted plant gains at 150 Hz and 188 Hz are significantly larger for the upper bearing. As shown earlier in Figure 7, the AMB damping at both the upper and lower ends of the rotor is negative in this frequency range. The upper bearing instability can be attributed to an unstable rigid-body mode when the AMB is attempting to levitate the rotor while the rotor is forced against the auxiliary bearings.

Periodicity of Impulses

Further review of the data showed that the rotor speed decreased by approximately 200 rpm at approximately the same time as the rotor contact with the lower auxiliary bearing. To gain insight into this phenomenon, a current probe was connected to one of the motor leads and several hours of motor current data were recorded and examined. Figure 13 shows the motor current vs. time for a particular 7.5-hour run. It was discovered that there was a large, periodic impulse overloading the motor approximately every 55 minutes.

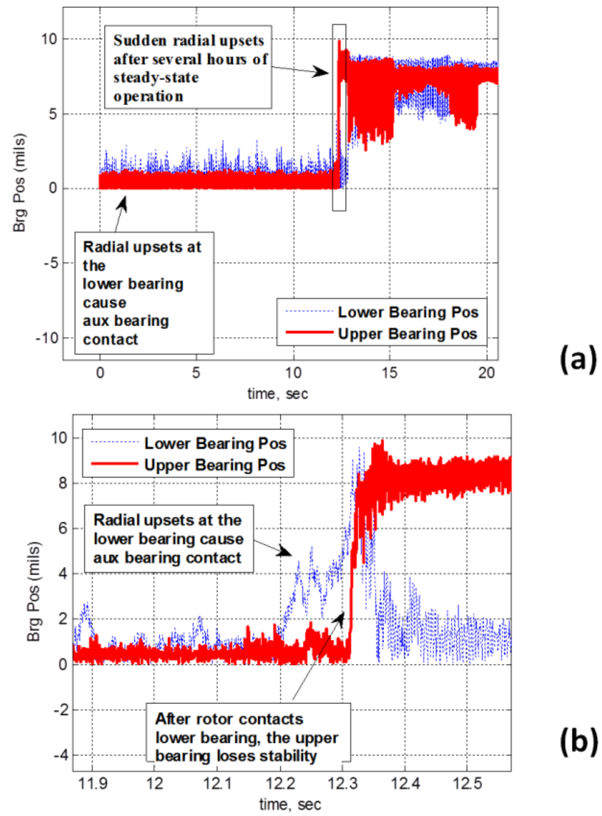

Figure 11. Rotor position magnitude before, during, and after a drop; (a) shows data across 30 seconds and (b) shows data across 0.7 seconds

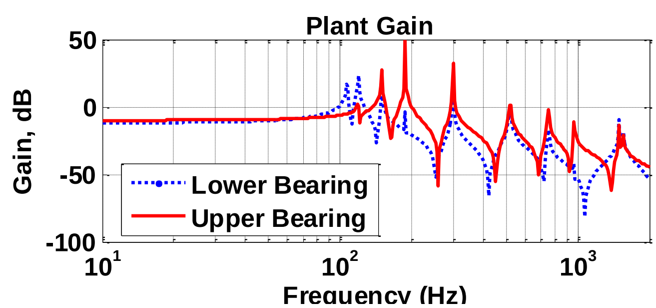

Figure 12. Predicted plant gain for the rotor supported by both the AMBs and the auxiliary bearings

The times at which each of these impulses occurred corresponded with the times at which the lower radial bearing position sensors detected large rotor excursions. All of the excessive vibration faults occurred at the same times as the motor impulses, but not all impulses were large enough to cause a trip due to an excessive vibration fault.

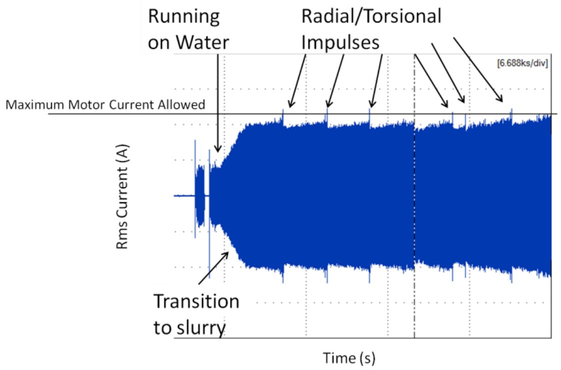

Figure 13. Motor current vs. time during a 7.5-hour run

Each vibration trip causes significant process downtime, ranging from 45 to 90 minutes. As such, a rudimentary re-levitation feature was incorporated into the MBC firmware to allow the atomizer to continue running without interruption to the process. The re-levitation feature drops the rotor after a loss of control is detected, and then attempts to re-levitate the rotor while it is still continuously spinning at the operating speed.

Generally speaking, approximately 75% of the rotor drops were successfully re-levitated using this feature without short-term interruption to the process. The auxiliary bearings were originally intended to withstand 10 full-speed rotor drops and spindowns. However, with the addition of the re-levitation feature, the rated life of the auxiliary bearings was extended to 35 drops, provided that the re-levitation attempts were continuously successful in preventing a full spindown of the rotor after a drop event. Even so, the auxiliary bearings were replaced approximately once per month due to the high frequency of impulse overload events.

In total, three MSM-250 V0 field test units were installed, all consistently experiencing the same problems. The major issues affecting the operability of the atomizer, all discovered during initial field testing of the MSM-250 V0 units, are summarized below:

(1.) Due to rotor flexibility, it was difficult to raise the stiffness of the lower radial AMB enough above the initial design value. This had two detrimental effects: a) the full load capacity of the lower radial AMB could not be applied before auxiliary bearing contact, and b) the rotor motion during steady-state operation did not allow a comfortable range of motion for impulse events.

(2.) Radial load impulse events large enough to cause auxiliary bearing contact and rotor drops occurred too frequently for sustained long-term operation of the atomizer.

(3.) Although the simple re-levitation feature worked well, it still resulted in repeated use and life reduction of the auxiliary bearings.

(4.) The root-cause of the radial impulses was attributed to the atomizing process, but was not well-understood.

DESIGN IMPROVEMENTS

Several changes were introduced to the MSM-250 V0 design to improve the performance of the atomizer. The primary goal of these design changes was to reduce the closed-loop response of the rotor in order to limit the total rotor motion during normal operation with slurry and to help withstand the large radial impulses impacting the disc. In order to gain more flexibility in the design of the compensator at low frequencies, the frequency of the first backward-whirl and forward-whirl bending mode needed to be increased well beyond the operating speed range. As mentioned earlier, the first bending mode frequency is primarily influenced by the stiffness of the lower bearing section and the mass/inertia properties of the disc.

Firstly, the design of the disc was optimized to reduce its weight from approximately 40 lbf (178 N) to 28 lbf (125 N). This reduction in weight shifted the first backward-whirl bending mode at 13,000 rpm up from 240 Hz to 271 Hz. The first forward-whirl bending mode at 13,000 rpm was shifted up from 477 Hz to 535 Hz.

To further increase the 1st bending mode frequencies, the auxiliary bearing size for the lower end of the rotor was increased from a 2.36 inch (60 mm) OD bearing to an 3.15 inch (80 mm) OD bearing, and as such, the OD of the rotor was also increased by 20 mm to maintain the same auxiliary bearing clearance. Figure 14 shows a comparison of the measured plant gains at 13,000 rpm for the MSM-250 V0 and V1 designs. For the V1 design, the first backward-whirl bending mode is at 342 Hz and the first forward-whirl bending mode is at 614 Hz, at 13,000 rpm.

Figure 15 shows a comparison of the AMB stiffness and damping characteristics for the MSM-250 V0 and V1 designs. The changes to the MSM-250 V1 rotor enabled the implementation of a stiffer AMB compensation at frequencies up to 200 Hz, while still maintaining robust stability margins.

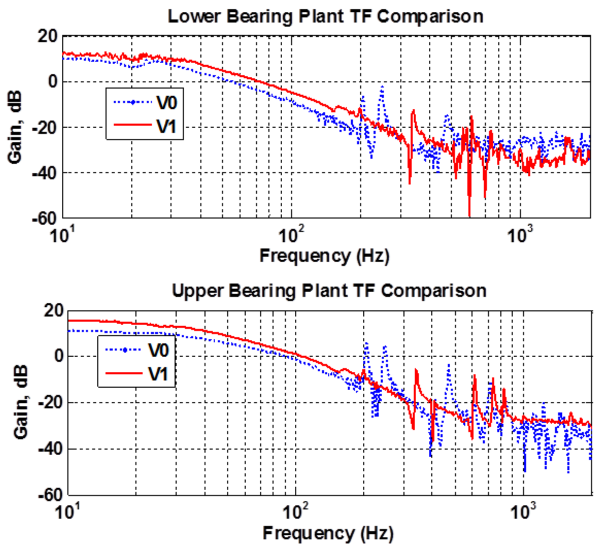

Figure 14. Lower and upper bearing plant magnitude response

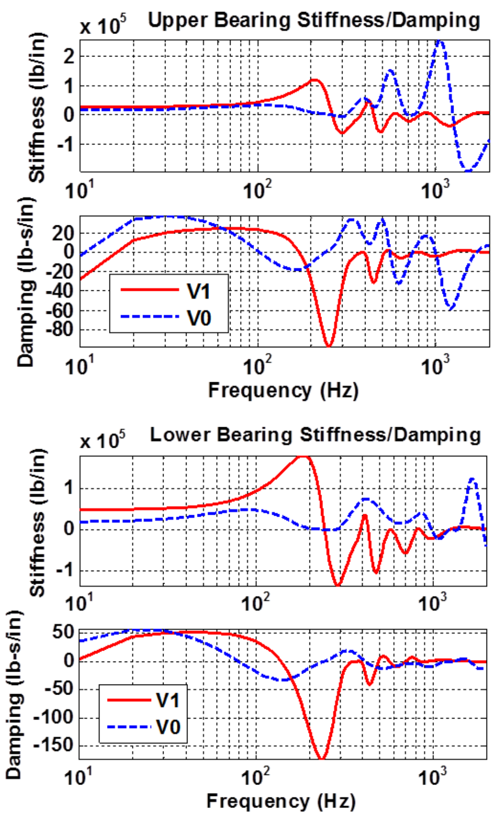

Figure 15. Comparison of the AMB stiffness and damping for the V0 and V1 designs

Figure 16 shows the difference in the measured closed-loop response for the V0 and V1 designs of the MSM-250. The closed-loop response for the V1 design is lower by a factor of 0.35 in the 10-20 Hz Hz frequency range. This means that for an externally-applied force in the 10-20 Hz frequency range, the response of the V1 rotor is 2.85 (1/0.35) times lower than that of the V0 rotor.

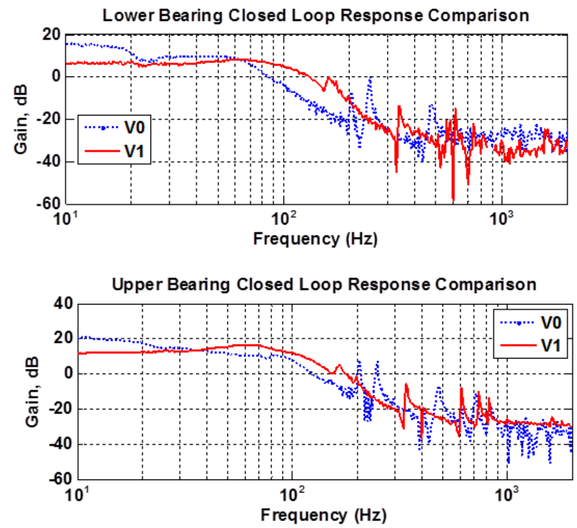

Figure 16. Comparison of the closed-loop response for the V0 and V1 designs

Figure 17 shows a comparison of the position orbits for the V0 and the V1 designs during an approximate 3-minute run on slurry. It is clear from the figure that the total rotor motion during steady-state operation is smaller for the V1 design.

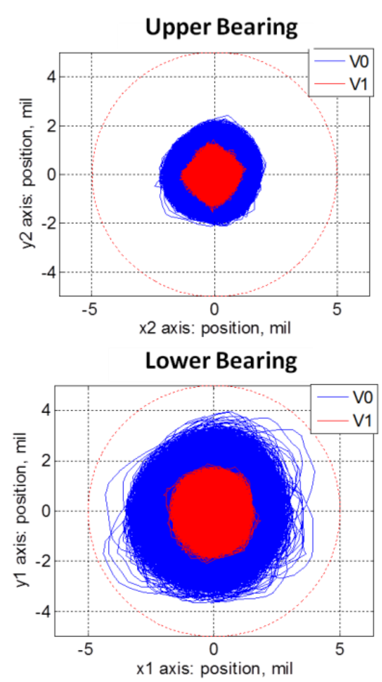

Figure 17. Comparison of position orbits for the V0 and V1 designs at the upper (top) and the lower (bottom) bearings

IMPULSE DETECTION AND RECOVERY FEATURE

A novel impulse detection and recovery feature was incorporated into the MBC firmware to allow for the AMBs to quickly recover the rotor in case of auxiliary bearing contact due to overloading of the AMBs. The IDR has four major steps:

(1.) Detect that a potential impulse event has occurred.
(2.) Switch the compensator to an "Impulse Recovery Compensator" (IRC), designed to stably levitate while in contact with the auxiliary bearings.
(3.) Wait for the rotor to recover. If the rotor recovers, switch back to the nominal compensator.
(4.) If the rotor does not recover, stop controlling the rotor, and then attempt a re-levitation.

Impulse Detection

Impulse detection is accomplished by continually monitoring the radial rotor position at both the upper and lower bearings, and the axial rotor position. The sampling frequency for this is 12500 Hz. When the rotor position increases beyond 4.75 mils (121 μm) radial on either bearing, or 6 mils (152.4 μm) axial, an impulse event will be declared.

Recovery Using IRC

After an impulse is detected, the MBC switches from using the nominal compensator to using the IRC. The IRC is designed to be stable when the rotor is levitated and when the rotor is pressed against the auxiliary bearings. To accomplish this, the IRC has a significantly reduced stiffness at low frequencies, and has lightly-positive damping up to approximately 400 Hz on both radial bearings. Figure 18 shows a comparison of the lower bearing stiffness and damping using the two different compensators.

Every time the IRC was triggered, it was logged by the MBC, and the IRC counter was incremented by 1. Figure 19 shows a log of the IRC counter from the first 24-hour run of the atomizer. The IRC was activated approximately every 49 minutes during this run, confirming the periodicity of the radial impulses seen earlier in the motor current data in Figure 13. During subsequent runs, the time between IRC events varied between 45 minutes and 80 minutes, but was consistent throughout each particular run.

At the time of this writing, the first MSM-250 V1 field test unit has run for approximately 1000 hours. During this time, the unit has tripped twice due to excessive synchronous vibration without successfully re-levitating. In both instances, slurry was found to have built up excessively on the atomizer disc over time, and had to be manually cleaned in order to continue operation. The two trips occurred within the 100 hours of each other, and are believed to be process-related anomalies at this time. The AMBs were able to recover the rotor after all other radial impulses. If this rate holds, the auxiliary bearings would need to be replaced approximately once per year, a significant improvement over the V0 design.

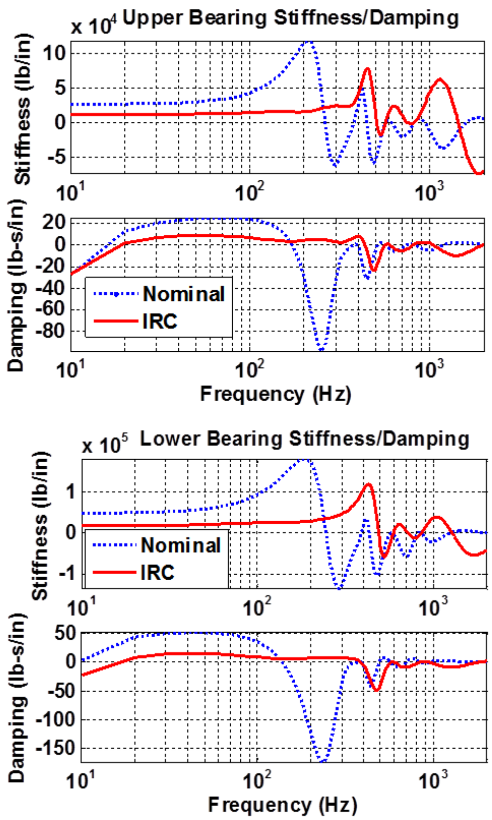

Figure 18. Comparison of the AMB stiffness and damping between the nominal compensator and the IRC compensator for the lower (a) and upper (b) bearings

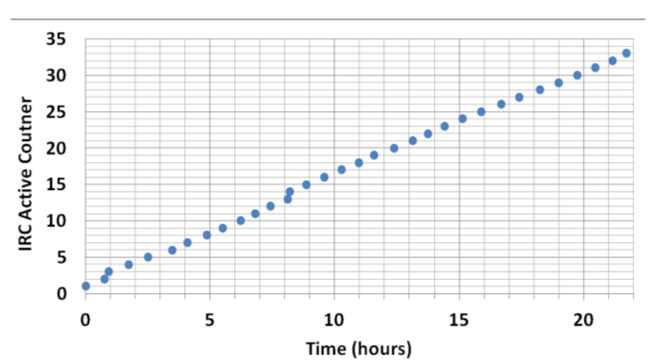

Figure 19. IRC counter vs. time showing periodicity of radial impulses

ONGOING INVESTIGATION AND FUTURE WORK

While the design and software improvements described above are significant steps towards resolving the process-related challenges imposed on the AMBs, the root cause behind the large, periodic radial impulses seen at the atomizer disc remains an item of ongoing investigation. The impulses could possibly be due to large, dense material passing through to the atomizer or large, uneven buildups and discharges of material on the disc. An effort is being made to both understand and reduce the frequency and severity of these radial impulses.

In an attempt to decrease the frequency of the radial impulses, a strainer has been placed near the inlet of the atomizer feed tubes. The effectiveness of the strainer is still under investigation. The authors are also currently investigating the effects of reducing the coefficient of friction on the disc surface. The authors are evaluating various methods of coating and/or polishing the disc to limit the buildup of dried slurry. At this time, a durable and effective coating or polishing method has not been identified.

Between November 2014 and November 2015, four more MSM-250 V1 units will be installed in a similar application to the one described in this paper. Additionally, in July 2015, the MSM-250 V1 will be placed in an application using a slurry with a viscosity <1 Pa-s.

SUMMARY AND CONCLUSIONS

A prototype design (V0) and an improved design (V1) for a rotary-disc atomizer driven by a permanent-magnet motor supported by AMBs have been presented. During initial testing of the V0 design, it was observed that the rotor was being subjected to occasional impulse forces large enough to overload the AMBs. Four major problem areas were identified with the V0 design:

(1.) Low AMB stiffness
(2.) Too many rotor drops
(3.) Too many unsuccessful re-levitations
(4.) Lack of understanding behind the root cause of the radial impulses

The V1 design was introduced to address three of the four problem areas. Field data shows that the V1 design has a considerably lower closed-loop response than the V0 design. This, in turn, reduces the total radial motion of the rotor during normal, steady-state operation of the atomizer, especially at the lower bearing. All of this has reduced the sensitivity of the V1 machine to radial impulses compared to the V0 design. A novel impulse detection and recovery feature has been implemented into the MBC's firmware, and it has been shown to substantially increase the probability of maintaining or recovering rotor levitation during or after an AMB overload. Although the V1 design has provided a workable solution to the process-related challenges described in this paper, there is an ongoing effort to further understand and mitigate the process-related radial impulses impacting the atomizer disc.

REFERENCES

[1] Bazergui, C., "Rotary Atomizer Having Electro-Magnetic Bearings and a Permanent Magnet Rotor", Patent Application No. 20130015264, Dedert Corporation, January, 17, 2013

[2] Filatov et al., "An Axial Position Sensor for Active Magnetic Bearings", ASME Turbo Expo 2010, Paper GT2010-22524, June 14-18, Glasgow, UK

[3] A. Filatov, L. Hawkins, "Novel Combination Radial/Axial HomopolarActive Magnetic Bearing", *Proceedings of the 1st Brazilian Workshop on Magnetic Bearings*, Rio-De-Janeiro, Brazil, 2013.

[4] Hawkins et al., "Development of a 125kw AMB Expander/Generator for Waste Heat Recovery", ASME Turbo Expo 2010, Paper GT2010-22763, June 14-18, Glasgow, UK

[5] Schweitzer, G., Maslen, E.H, 2009, *Magnetic Bearings: Theory, Design, and Application to Rotating Machinery*, Springer Verlag, Berlin, Germany, pp. 288-294.

[6] Hawkins et al., "Test Results and Analytical Predictions for Mil-Std-167 Vibration Testing of a Direct Drive Compressor Supported on AMB", ASME Turbo Expo 2014, Paper GT2014-25366, June 16-20, Düsseldorf, Germany

[7] Smalley, A.J., et al, "The Dynamic Characteristics of O-Rings," Transactions of the ASME, Vol 100, pp 132-138, January, 1978